Reliability Analysis of a Bridge Deck Utilizing Generalized Gamma Distribution

Muyang Lu[1]; Jonathan Hydock[2]; Aleksandra Radlińska, Ph.D., A.M.ASCE[3]; and S. Ilgin Guler, Ph.D., A.M.ASCE[4]

Abstract: Models of bridge deck deterioration with improved predictive power can provide bridge management strategies that will optimize allocation of the available, typically limited, budget of transportation agencies in a more efficient manner. In turn, this will lead to improvement in the overall condition of bridges. To this end, this study developed a novel statistical hazard model of bridge deck deterioration using a generalized gamma accelerated failure time model with bridge deck attributes as covariates. Bayesian inference was used to estimate the parameters of the model and will update these parameters as new inspection data become available. The Markov chain Monte Carlo sampling method was used to estimate the posterior distribution of parameters utilizing both uncensored and censored inspection data. The proposed approach was applied to approximately 30 years of in-service performance data inspected from 1985 to 2015 for more than 22,000 bridges in the state of Pennsylvania. The results showed that the model based on the generalized gamma distribution had a high accuracy. Further, the reliability of different attribute values of the physical makeup of the main span of the structure, the main span interaction type, and the rebar coating are quantified based on the model results. The proposed model can help improve predictions of future bridge deck conditions and provide decision-making tools for infrastructure management. **DOI:** 10.1061/(ASCE)BE.1943-5592.0001842.

Author keywords: Bridge deck deterioration; Survival probability; Generalized gamma distribution model; Bayesian updating; MCMC sampling.

Introduction

Bridge deck safety is critical to the safety and well-being of the public; however, bridge decks continuously deteriorate over their lifetime. This process is influenced by various factors, such as the attributes of the bridge deck, the surrounding environment, and the truck traffic. Pennsylvania has more than 25,000 state-owned bridges, and in 2018, PennDOT spent 18.3% of its revenue on the Highway & Bridge Maintenance program, with 29.9% of that being spent only on the improvement of bridge decks (PennDOT 2019). PennDOT performs about 18,000 bridge safety inspections every year, and each bridge is inspected approximately every 2 years and assigned a condition rating (CR) for the bridge deck, superstructure, substructure, culvert, and overall condition. This inspection data set can be used to explore significant attributes that influence the deterioration process and develop decision-making tools for bridge deck maintenance and rehabilitation planning.

[1]Ph.D. Student, Civil and Environment Engineering, Pennsylvania State Univ., 406B Sackett Building, University Park, PA 16802 (corresponding author). ORCID: https://orcid.org/0000-0001-6687-6986. Email: muyang@psu.edu

[2]B.S. Student, Civil and Environment Engineering, Pennsylvania State Univ., 231D Sackett Building, University Park, PA 16802. Email: jonathanhydock@gmail.com

[3]Associate Professor, Member ASCE, Civil and Environment Engineering, Pennsylvania State Univ., 231D Sackett Building, University Park, PA 16802. ORCID: https://orcid.org/0000-0002-7977-4927. Email: azr172@psu.edu

[4]Assistant Professor, Member ASCE, Civil and Environment Engineering, Pennsylvania State Univ., 231J Sackett Building, University Park, PA 16802. Email: iguler@engr.psu.edu

Note. This manuscript was submitted on March 22, 2021; approved on December 3, 2021; published online on January 27, 2022. Discussion period open until June 27, 2022; separate discussions must be submitted for individual papers. This paper is part of the ***Journal of Bridge Engineering***, © ASCE, ISSN 1084-0702.

Literature Review

Stochastic Deterioration Models

Many infrastructure deteriorations models have been proposed in the existing literature and generally can be split into two categories: deterministic and probabilistic methods (O'Leary et al. 2012; Zhang and Durango-Cohen 2014; de Melo e Silva et al. 2000). While deterministic methods are simple and intuitive, their accuracy highly depends on the adequacy and comprehensiveness of the data. Extrapolating results from deterministic models can lead to incorrect results (de Melo e Silva et al. 2000; Black et al. 2005). On the other hand, probabilistic methods are more realistic for prediction of asset deterioration, which are probabilistic, not deterministic, in nature. Markovian chain Monte Carlo (MCMC) modeling is the most commonly used stochastic approach. Markov models can closely capture the uncertainty in the infrastructure deterioration process, but the assumption that the time spent in the current condition state does not affect the probability of moving to the next state, named the memoryless property, is a typical concern (Butt 1991; Mishalani and Madanat 2002). Therefore, the semi-Markov process that allows the transition probability to be dependent on the time spent in any given state has been more widely used for infrastructure deterioration modeling over the last two decades (Agrawal et al. 2010; Sobanjo 2011; Thomas and Sobanjo 2013; Manafpour et al. 2018). Howard (2007) presented the probability that a continuous-time semi-Markov process will be in state j at time t given that it entered state i at time zero, $\phi_{ij}(t)$, as

$$\phi_{ij}(t) = \delta_{ij} w_i(t) + \sum_{k=1}^{N} \int_0^t H_{ik}(\tau)\phi_{kj}(t-\tau)d\tau \quad i, \\ j = 1, 2, \ldots, N; t = 0, 1, 2, \ldots \tag{1}$$

where δ_{ij} = Kronecker delta (i.e., $\delta_{ij} = 1$ if $i = j$ and $\delta_{ij} = 0$ otherwise); $w_i(t)$ = probability that the process will leave its starting

state i at a time greater than t; N = number of all possible states; and H_{ik} = probability of transitioning from state i to k at time τ, also known as the semi-Markov kernel or the hazard function. The hazard function, $H_{ik}(\tau)$, reflects the reliability of the infrastructure and can take any bathtub-shape distribution. For example, when the exponential distribution is chosen for the hazard model, the semi-Markov process reduces to a traditional Markov process. Sobanjo (2011) suggested that the choice of $H_{ik}(\tau)$ is crucial to the process of accurate modeling of the sojourn times.

Distributions of Hazard Function Used for Reliability Modeling

Different statistical distributions for the hazard, such as exponential, gamma, and Weibull, have been used in the field of reliability (Kobayashi et al. 2010; Tabatabai et al. 2011; Barone and Frangopol 2014; Nasrollahi and Washer 2015). Weibull distribution is most commonly used in the literature to fit the distribution of bridge or pavement deterioration. Sobanjo et al. (2010) compared Weibull, lognormal, and exponential distribution when modeling a bridge superstructure's deterioration process and found that the Weibull distribution achieved the best performance measured by the Anderson–Darling test.

However, it is difficult to model real data with these more limited distributions since the data do not necessarily fit the shape of these distributions (Agarwal and Kalla 1996). Thus, the generalized gamma distribution (GGD) was introduced into reliability theory to extend the useful scope of the ordinary gamma and Weibull distributions and to allow modeling of more flexible distribution shapes (Agarwal and Kalla 1996). The GGD distribution was first described in 1965 (Stacy and Mihram 1965; Cohen and Whitten 2020) and can be reduced to nearly all of the most commonly used distributions, including the exponential, Weibull, log normal, and gamma distributions (Hirose 2000). More importantly, it can model all four of the most common types of hazard functions: monotonically increasing and decreasing, as well as bathtub and arc-shaped hazards (Stacy and Mihram 1965; Cox et al. 2007; de Pascoa et al. 2011). However, this increased flexibility requires that more parameters be estimated, which in turn makes the estimation process more complex (Kleiber and Kotz 2003). Several approaches have been proposed to estimate these parameters, such as maximum likelihood estimation (Hirose 2000; de Pascoa et al. 2011), method of moments (Kleiber and Kotz 2003), heuristic methods (Gomes et al. 2008), or Bayesian inference (Bayes and Branco 2007; de Pascoa et al. 2011; Yang et al. 2018).

Bayesian Updating and MCMC Methods

Bayesian inference can achieve an accuracy equivalent to maximum likelihood estimation but can also provide the intervals for the parameter estimates that can allow for risk analysis or updating of parameters as new data become available. Enright and Frangopol (1999) considered combining a data-driven model based on the lognormal distribution with expert knowledge using Bayesian updating. Taflanidis and Gidaris (2013) implemented Bayesian updating for bridge deterioration assuming the data follow a Gaussian distribution. Beck and Au (2002), Hsein Juang et al. (2013), and Straub and Papaioannou (2015) developed a Bayesian updating approach for structural reliability modeling and implemented the MCMC algorithm to estimate the parameters considering Gaussian, lognormal, and beta distributions. Bayesian updating is efficient, but the accuracy of the predictive models depends highly on the assumed distribution. The flexibility of GGD to fit the data, combined with the Bayesian estimation, can allow for this method to provide accurate estimations for deterioration modeling. While this powerful distribution has been applied in the medical science and material fatigue fields (Agarwal and Kalla 1996; Manning et al. 2002), it has not been utilized in the infrastructure deterioration process, especially when considering covariates.

Covariate's Analysis

These distribution-based reliability models have aimed at determining the sojourn time; however, in practice, the bridge deck-deterioration process is influenced by various covariates, such as the structure of the bridge, the overlay material, and the rebar type. To incorporate the impacts of covariates in deterioration models, different approaches have been used in the literature. Some researchers have built predictive models for bridges grouped into several categories based on different attributes, which increased the complexity of the model and ignored the dependency between different attributes (Sobanjo et al. 2010). A more common way to incorporate the covariates into one model has been the proportional hazards (Cox et al. 2007; Zhu et al. 2015) or accelerated failure time models (Wei 1992; Tabatabai et al. 2011; Manafpour et al. 2018). These approaches either scale the hazard by a function of the covariates or assume that a parametric regression model is used for the reliability analysis. The latter approach has an intuitive physical interpretation and is also simple to apply for commonly used reliability distributions.

Research Objectives

To extend the existing distribution-based deterioration models that incorporate covariates, this study adopted the generalized gamma distribution to the bridge deck reliability analysis considering the impact of covariates for a given CR. An accelerated failure time (AFT) generalized gamma distribution (GGD)-based deterioration model was proposed that can incorporate the impacts of significant attributes that influence the bridge deck deterioration. A corresponding Bayesian inference approach was suggested to estimate the parameters and their possible ranges. An application of these ranges was shown for updating the models as new inspection data become available; however, these ranges are also useful when determining asset management strategies considering different risk levels. This approach was demonstrated using 30 years of in-service performance data for more than 22,000 bridges in Pennsylvania. The remainder of the paper is organized as follows: the section "Methodology" introduces the AFT–GGD model along with the Bayesian inference algorithm, followed by the section "Data Description", which discusses the Pennsylvania-based real-life data, and the "Results" section shows the results of the model estimation. Finally, concluding remarks are presented in "Conclusions".

Methodology

The goal of this paper is to conduct a survival analysis of the duration that a bridge deck spends in a given CR to better account for the variability in the inspection data. For these models, the time a bridge deck lasts in each CR or cumulative truck traffic in a given CR was considered as the independent variable. These variables were modeled assuming they follow a generalized gamma distribution using an accelerated failure time approach to incorporate the covariates. The parameters of this model were estimated using MCMC methods based on Bayesian theory that can provide ranges of confidence for the results, and can update the parameters

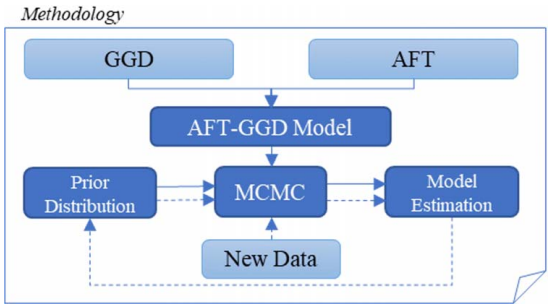

Fig. 1. Flow chart of the methodology.

as new data become available, without re-estimating the entire model. A flowchart of the methodology can be seen in Fig. 1. The main steps of the methodology are discussed next.

Accelerated Failure Time, Generalized Gamma Distribution Model

Survival analysis aims at modeling the sojourn time, defined as the duration of time or traffic load until an event, or failure, happens. The specific dependent variable being modeled in a survival analysis is known as the "hazard," which is defined as the probability of failure at a given time conditional on the fact that failure has not happened until that time. The hazard rate function $H(t)$ can be defined as

$$H(t) = \frac{f(t)}{R(t)} \tag{2}$$

where $f(t)$ = probability density function of the sojourn time defined as the probability that an event lasts at least until time t; and $R(t)$ = reliability (or the survival) function of the sojourn time.

Accelerated failure time models assume that the covariates accelerate or decelerate the failure time. In this study, accelerated failure time models were chosen due to their flexibility. The general form of an accelerated failure time model assumes that the logarithm of the failure time can be expressed as a linear function of covariates as

$$\log(t) = \boldsymbol{\beta x} + \varepsilon \tag{3}$$

where $\boldsymbol{x} = [1, x_1, x_2, \ldots, x_k]$ = vector of covariates; $\boldsymbol{\beta} = [\beta_0, \beta_1, \beta_2, \ldots, \beta_k]$ = vector of the coefficients of covariates; k = number of covariates; β_0 = constant term; and ε = random error term with a given probability distribution function. The covariates were assumed to be independent of each other since they represent different attributes of bridge decks that are typically chosen independently in practice. This assumption was further checked and found to be appropriate by considering the correlation between the posterior distribution of the coefficients (see the "Results" section).

The distribution of the random error determines the resulting shape of the hazard and reliability function. In this paper, the error term was assumed to follow the GGD. The steps to modify the AFT methodology to represent a GGD are described in the Appendix. Following this methodology, the PDF of the AFT–GGD can be written as

$$f(t, \boldsymbol{x}|\sigma, \lambda, \boldsymbol{\beta}) = \begin{cases} \dfrac{|\lambda|}{\sigma t}\dfrac{1}{\Gamma\left(\dfrac{1}{\lambda^2}\right)} e^{\left[\dfrac{\lambda\dfrac{\ln(t)-e^{\boldsymbol{\beta x}}}{\sigma} + \ln\left(\dfrac{1}{\lambda^2}\right) - e^{\lambda\dfrac{\ln(t)-e^{\boldsymbol{\beta x}}}{\sigma}}}{\lambda^2}\right]} & \lambda \neq 0 \\ \dfrac{1}{t\sigma\sqrt{2\pi}} e^{-\dfrac{1}{2}\left(\dfrac{\ln(t)-e^{\boldsymbol{\beta x}}}{\sigma}\right)^2} & \lambda = 0 \end{cases} \tag{4}$$

where σ, λ, and $\boldsymbol{\beta}$ = parameters of the AFT–GGD model.

Estimating the Parameters

There are several approaches to estimate the parameters of the model, σ, λ, and $\boldsymbol{\beta}$, including maximum likelihood estimation (MLE) and Bayesian inference. As discussed in the Introduction section, Bayesian inference can achieve an equivalent accuracy as MLE while providing more detailed estimation results, including confidence intervals. Further, this estimation approach can allow the model to be updated when new data become available, without re-estimation of the whole model. Thus, a parameter estimation approach based on Bayesian inference was designed in this study to estimate the parameters of the model. The process of Bayesian inference can be described as

$$f_X(\sigma, \lambda, \boldsymbol{\beta}|D) = k \times f_X(\sigma, \lambda, \boldsymbol{\beta}) \times L(D|\sigma, \lambda, \boldsymbol{\beta})$$

$$\propto f_X(\sigma, \lambda, \boldsymbol{\beta}) \times L(D|\sigma, \lambda, \boldsymbol{\beta}) \tag{5}$$

where $f_X(\sigma, \lambda, \boldsymbol{\beta}|D)$ = probability density function (PDF) of posterior distribution of the parameters after observing data D; $f_X(\sigma, \lambda, \boldsymbol{\beta})$ = PDF of the prior distribution of the parameters, and when prior information is not available, it is the joint distribution of σ, λ, and $\boldsymbol{\beta}$ determined based on prior knowledge or engineering judgement; $L(D|\sigma, \lambda, \boldsymbol{\beta})$ = likelihood function that data D is observed given σ, λ, and $\boldsymbol{\beta}$; and k = normalizing constant.

The likelihood function was composed of two parts, depending on the type of available data: (1) the likelihood function of the uncensored data, that is, data where the observation period covers both the beginning and the end of a condition rating, which can be calculated as the probability density function; and (2) the likelihood function of censored data that is, either the beginning or the end of a condition or both is not observed and can be calculated using the reliability function. Thus, the final likelihood function

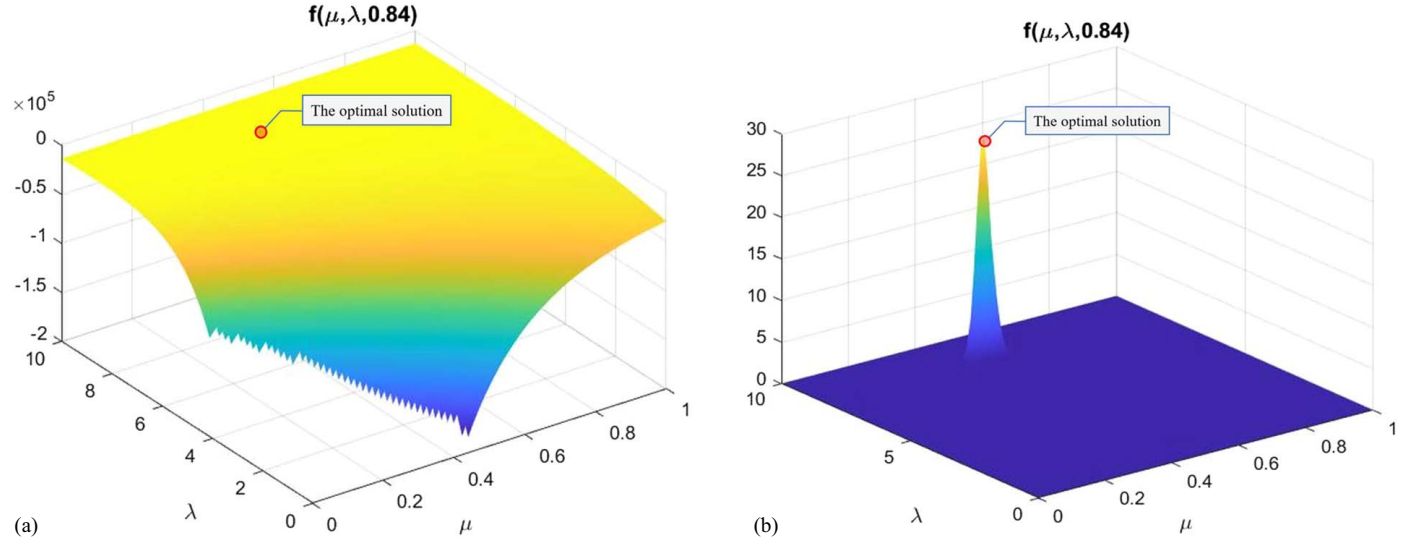

Fig. 2. Likelihood distribution of the generalized gamma distribution: (a) before likelihood transformation; and (b) after likelihood transformation.

of the whole data set could be expressed as a product of the probability density functions of the uncensored data and the reliability functions of the censored data as

$$L(D|\sigma, \lambda, \boldsymbol{\beta}) = \prod_{t_i \in D_u} f(t_i|\sigma, \lambda, \boldsymbol{\beta}) \prod_{t_i \in D_c} R(t_i|\sigma, \lambda, \boldsymbol{\beta}) \tag{6}$$

where D_u = data set of all uncensored data; D_c = data set of all censored data; f = probability density function; and R = reliability function.

When there was no prior information, the prior distribution was determined as the joint distribution of σ, λ, and $\boldsymbol{\beta}$, which was assumed to follow uniform distribution in this study, as

$$\sigma \sim U(a_\sigma, b_\sigma), \lambda \sim U(a_\lambda, b_\lambda), \beta_i \sim U(a_{\beta_i}, b_{\beta_i}) \tag{7}$$

where β_i = elements of $\boldsymbol{\beta}$; and a_*, b_* = hyper-parameters of the prior distribution, which can be initialized based on experience. Thus, the PDF of prior distribution when there was no prior information was calculated as

$$f_X(\sigma, \lambda, \boldsymbol{\beta}) = \frac{1}{b_\sigma - a_\sigma} \times \frac{1}{b_\lambda - a_\lambda} \times \prod_i \frac{1}{b_{\beta_i} - a_{\beta_i}} \tag{8}$$

When a model already exists, the posterior distribution calculated using the previously available data, $f_X(\sigma, \lambda, \boldsymbol{\beta}|D)$, became the prior distribution for the new model, $f_X(\sigma, \lambda, \boldsymbol{\beta})$.

MCMC Sampling

An analytical expression for the posterior distribution function [Eq. (4)] does not exist. The MLE for GGD, especially when modified by an AFT approach to incorporate covariates, is complex. Hence, the distribution of the parameters σ, λ, and $\boldsymbol{\beta}$ must be estimated using a heuristic algorithm or sampling approach. Here, a standard Metropolis–Hasting MCMC (MH–MCMC) method was used. The MCMC method provides more flexibility and additional useful information than the MLE and Kaplan–Meier (K–M) method. First, the MCMC generates samples form the entire posterior, and therefore provides more accurate and reliable estimations than the MLE and K–M estimator. These samples can be used for updating the parameters as prior distribution samples directly. This is helpful especially when the type of posterior distribution is not normal distribution and is hard to fit to a known distribution.

In the MH–MCMC sampling process, an initial sample consisting of σ, λ, and $\boldsymbol{\beta}$ was generated using Eq. (7). Further, this set of parameters was used to determine the corresponding likelihood and posterior probability, $f_X(\sigma, \lambda, \boldsymbol{\beta})$, using Eqs. (6) and (5), respectively. Next, a second sample, $(\sigma', \lambda', \boldsymbol{\beta}')$, was generated around the initial sample with a normally distributed transition probability, $p(\sigma', \lambda', \boldsymbol{\beta}'|\sigma, \lambda, \boldsymbol{\beta})$, known as "proposal distribution," and again the posterior probability was calculated. Then, the transition probability from $(\sigma', \lambda', \boldsymbol{\beta}')$ back to $(\sigma, \lambda, \boldsymbol{\beta})$ was calculated with the proposal distribution as $p(\sigma, \lambda, \boldsymbol{\beta}|\sigma', \lambda', \boldsymbol{\beta}')$. Finally, the MH–MCMC method determines whether to accept this new sample or to continue with the initial sample. The new sample is accepted with probability, α, as

$$\alpha = \min\left(1, \frac{f_X(\sigma', \lambda', \boldsymbol{\beta}')p(\sigma, \lambda, \boldsymbol{\beta}|\sigma', \lambda', \boldsymbol{\beta}')}{f_X(\sigma, \lambda, \boldsymbol{\beta})p(\sigma', \lambda', \boldsymbol{\beta}'|\sigma, \lambda, \boldsymbol{\beta})}\right) \tag{9}$$

This acceptance ratio was chosen to ensure that samples with higher PDF values of posterior distribution were more likely to be accepted, thus allowing the samples to cluster around the optimal point. A Markov chain was thus generated by repeatedly drawing samples around the optimal point.

Addressing Computational Issues

There are some computational limitations to estimating the previously described model specifically for large data sets. Three major concerns are: (1) the likelihood function approaches zero as the likelihood for more data is considered, (2) the likelihood function is mostly flat around the optimal solution, and (3) the AFT–GGD approaches infinity when λ, μ are small. The modifications to the model to address these issues are discussed next.

Likelihood Function

As the number of available data increases, the likelihood value goes to 0 and the log-likelihood value to negative infinity. This results in the MCMC method failing to converge. See, for example, Fig. 2, which shows the likelihood distribution as a function of μ and λ while keeping σ constant for an illustration of this problem.

From Fig. 2(a), it can be observed that: (1) when λ or μ decreases, the likelihood function approaches negative infinity, and (2) the likelihood function is flat around the optimal solution (shown by the circle as estimated by maximum likelihood

estimation). When λ and μ approach zero, the computational effort becomes too large to determine the likelihood distribution. Since the optimal parameters should yield a computable log-likelihood value, the optimal solution would not be located in this region. The parameter combinations around the optimal solution are calculatable and remain stable. Both of these issues hinder the ability of the MCMC method to converge. Hence, the likelihood function was transformed into a logarithmic space as

$$\text{Log\_}L = \sum_{t_u \in D_u} \log(f(t_u)) + \sum_{t_c \in D_c} \log(f(t_c)) \tag{10}$$

Next, the maximum log-likelihood value for all parameters was calculated and subtracted from the log-likelihood value. Finally, the following likelihood function was used in the MCMC calculations as

$$L = \exp\left(\text{Log\_}L - \max_{\forall \mu,\sigma,\lambda}(\text{Log\_}L)\right) \tag{11}$$

Gamma Function

In the PDF function of the GGD shown in Eq. (4), when λ approaches 0, $1/\lambda^2$ starts approaching infinity, and the gamma function may overflow. Tests had shown that when λ is less than 0.05, the gamma function will overflow in any common programming language (i.e., Python, MATLAB).

To overcome this overflow problem, the function shown in Eq. (4) was transformed. First, the gamma function can be calculated as

$$\Gamma\left(\frac{1}{\lambda^2}\right) = e^{\log\left(\Gamma\left(\frac{1}{\lambda^2}\right)\right)} = e^{\sum_{i=1}^{k} \log\left(\frac{1}{\lambda^2}-i\right)+\log\left(\Gamma\left(\frac{1}{\lambda^2}-k\right)\right)} \tag{12}$$

Using Eq. (12) and substituting it in Eq. (4), the PDF can be transformed as (when $\lambda \neq 0$):

$$f = \frac{|\lambda|}{\sigma t} e^{\left[\frac{\lambda\frac{\ln(t)-e^{\beta x}}{\sigma} + \ln\left(\frac{1}{\lambda^2}\right) - e^{\lambda\frac{\ln(t)-e^{\beta x}}{\sigma}}}{\lambda^2} - \sum_{i=1}^{k}\log\left(\frac{1}{\lambda^2}-i\right) + \log\left(\Gamma\left(\frac{1}{\lambda^2}-k\right)\right)\right]} \tag{13}$$

The new plot of the likelihood function after this transformation is shown in Fig. 2(b). With this transformation, nonoptimal solutions had a likelihood value close to zero, including the areas that approached negative infinity in Fig. 2(a). Conversely, the optimal solution had a likelihood value that was distinctly higher than the surrounding values, while keeping the same optimal solution. Hence, through these two modifications the computational efficiency of the MCMC method was improved.

Data Description

The data set analyzed in this work consists of biannual inspections of bridges across Pennsylvania obtained from PennDOT. Historical bridge deck CR, along with attributes of the bridge structure obtained from the Bridge Management System (BMS2) (Pennsylvania 2009), were accessed for more than 22,000 bridge decks constructed between 1840 and 2015. These bridges were inspected between 1985 to 2015. Table 1 summarizes the available attributes from BMS2.

The inspection data were first pre-processed and cleaned as follows:

- If a CR increased or decreased for only a single inspection and returned to the previous CR in the next inspection, this data point was corrected to match the before and after condition rating.
- Data that did not have an inspection date were discarded.
- Data from bridges where a CR was not recorded for two consecutive inspections point were discarded (to eliminate possible errors in CR reporting).
- If there were more than 1,500 days (4 years) between two consecutive inspections points and the CR changed between these inspections, this data point was discarded (since the actual deterioration time would be unknown).
- If the CR changed more than two levels (higher or lower) between inspections, this change was marked as "sharply increased" or "sharply decreased," respectively. These data were treated as censored, and an indicator variable "EVENT" was included for these data as 1, or otherwise 0. A sudden increase could be due to a maintenance or reconstruction activity, and a sudden decline could be due to an incident happening on the bridge causing it to deteriorate quickly in a short time.

After cleaning the raw data, valid information for 18,354 bridges was obtained, and a total of 44,086 sojourn times were extracted and classified given the CR. To choose a suitable model to predict the life cycle performance of bridge decks, a nonparametric analysis of these sojourn times was first conducted. First, summary statistics for the distribution of the sojourn times were determined, as listed in Table 2.

Looking at Table 2, it can be observed that only a small number of bridges deteriorate to CR 3 or worse, as typically when a deck enters CR 3, it is designated for maintenance repair, rehabilitation, or replacement and/or CR 3 signifies nearing the end of the useful service life. Due to the lack of data for CRs 3, 2, and 1, this paper only utilizes data for bridge decks with a CR greater than 3.

Results

Considering the complexity of the full model and the limitation of the data set, the performance of the proposed model was first evaluated using a reduced model, which incorporates only one attribute, for example, rebar type, as a covariate. The reduced model was used to: (1) determine the appropriate dependent variable, (2) verify that the AFT–GGD model can fit the data better than other commonly used distributions, and (3) verify the accuracy of the MCMC estimation compared with maximum likelihood estimation. Next, a full model where all attributes that were considered was estimated. The influence of different attributes on the deterioration ratio were also analyzed. The applicability of the Bayesian updating method was demonstrated, and the parameter sensitivity was analyzed using the full model.

Table 1. Attributes description and values distribution

Discrete attributes	Description	Values (count)*
DISTRICT	District number	District 1 (2,707); District 2 (2,102); District 3 (3,171); District 4 (2,200); District 5 (2,215); District 6 (2,912); District 8 (5,369); District 9 (3,497); District 10 (2,443); District 11 (2,672); District 12 (2,817);
DEPT_DKSTRUC_TYP	Deck structure type	Concrete, reinforced (26,324);
DEPT_MAIN_MATERIAL_TYPE	Main materials type	Steel (8,531); concrete (cast in place) (6,205); concrete (precast) (537); prestressed precast concrete (P/S) (15,774); concrete-encased steel (982);
DEPT_MAIN_PHYSICAL_TYPE	Physical makeup of main span of structure	Reinforced (6,744); pretensioned (15,600); rolled sections (4,787); rolled sections with cover plates (1,174); combination, rolled sections/cover plates (334); other (3,313);
DEPT_MAIN_SPAN_INTERACTION	Span interaction for main span of structure.	Simple, noncomposite (12,042); simple, composite (15,377); continuous, noncomposite (882); continuous, composite (2,751); other (1,053);
DEPT_MAIN_STRUC_CONFIG	Structural configuration for main span of structure.	Slab (solid) (2,378); T beams (3,985); I beams (11,653); box beam, single (5,681); box beam, adj (6,614); I-welded beams (410); girder weld/deck (722);
DK_PROTECT	Deck protection type.	none (18,171); epoxy-coated reinforcing (12,439); galvanized reinforcing (461); unknown (804);
DECK_REBAR_TYPE	Deck rebar type.	bare rebar type (12,960); galvanized rebar type (561); epoxy rebar type (11,738); unknown (6,794);
MAIN_SPANS	Main bridge spans. (Number of spans in main unit.)	1 (20,209); 2 (4,954); 3 (4,167); 4 (1,416); 5 (585);
DKMEMBTYPE	Waterproofing membrane on bridge main span.	None (26,722); preformed fabric (3,816); other (368).
DKSURF_TYPE	Wearing surface types on bridge main span.	Concrete (14,137); concrete overlay (3,406); epoxy overlay (974); bituminous (13,340);
EVENT	If special event happened.	Sharply decrease (3,497); normal (22,332); sharply increase (6,212)

Continuous variables	Description	Mean	St. dev.	Min	Max
LENGTH	Bridge length (ft).	132.91	260.95	18	13,915
DECK WIDTH	Bridge deck width (ft).	35.56	603.83	11.50	187
ADTT	Average daily truck traffic (truck).	369.05	10.37	1	3,000

*The *Values (counts)* only show the values whose count is larger than 1% of the whole data set.

Table 2. Basic statistics of sojourn times of bridge decks

	Censored			Uncensored		
Condition rating	Count	Mean (days)	Std. (days)	Count	Mean (days)	Std. (days)
CR 1	19	2,809	2,509	2	1,040	348
CR 2	104	1,690	1,263	13	1,818	1,124
CR 3	1,007	2,022	1,709	170	2,034	1,421
CR 4	3,132	3,197	2,410	783	2,581	1,717
CR 5	6,016	4,010	2,759	2,317	2,935	1,794
CR 6	7,264	4,024	2,622	3,865	2,977	1,719
CR 7	8,636	3,957	2,603	3,817	3,054	1,760
CR 8	3,234	2,610	1,927	2,612	2,501	1,443
CR 9	654	1,420	1,106	381	1,747	1,049
Total		30,066			13,960	

The reduced model is only demonstrated for the deterioration process from CR 6 to CR 5, however, similar conclusions are drawn when considering deterioration from different condition ratings. The full model considered all the deterioration process from CR 9 to CR 4. In general, the MH–MCMC method was used to estimate the AFT–GGD model (unless specified otherwise) using 20,000 samples generated from the posterior distribution with a burn-in of 1,000 samples (i.e., the initial 1,000 samples were thrown away). The prior distribution was assumed to be uniform, with lower and upper limits of −10 and 10, respectively. This range was selected based on preliminary tests. The thinning was set as 2 since no significant autocorrelation was observed, which means that one sample was abandoned every two samples. After discarding burn-in samples and thinning, all coefficient samples of the MCMC followed a stable normal distribution for each attribute (e.g., rebar type).

Reduced Model, Models with a Single Covariate

Choice of Dependent Variable

Two candidate-dependent variables for modeling are available: (1) the time until the CR changes, that is, sojourn time; or (2) the total vehicle loading until the CR changes. Since the equivalent single-axle load of a car (which is directly related to the amount of damage done to the pavement) is negligible (FHWA 2016), in this paper, only truck traffic is used to represent traffic loading. Hence, the total vehicle loading is represented using the cumulative truck traffic (CTT), which was calculated by multiplying the time until a change in the CR and the average daily truck traffic. Both variables could predict deterioration of bridge decks; however, sojourn time and CTT evaluate the duration of a bridge from different perspectives. To evaluate the impact of different material type, how the reliability (or survival probability) would change for different bridge deck surface types was evaluated. The K–M estimator (Kaplan and Meier 1958) was used to calculate the reliability functions based on the uncensored and censored data. The

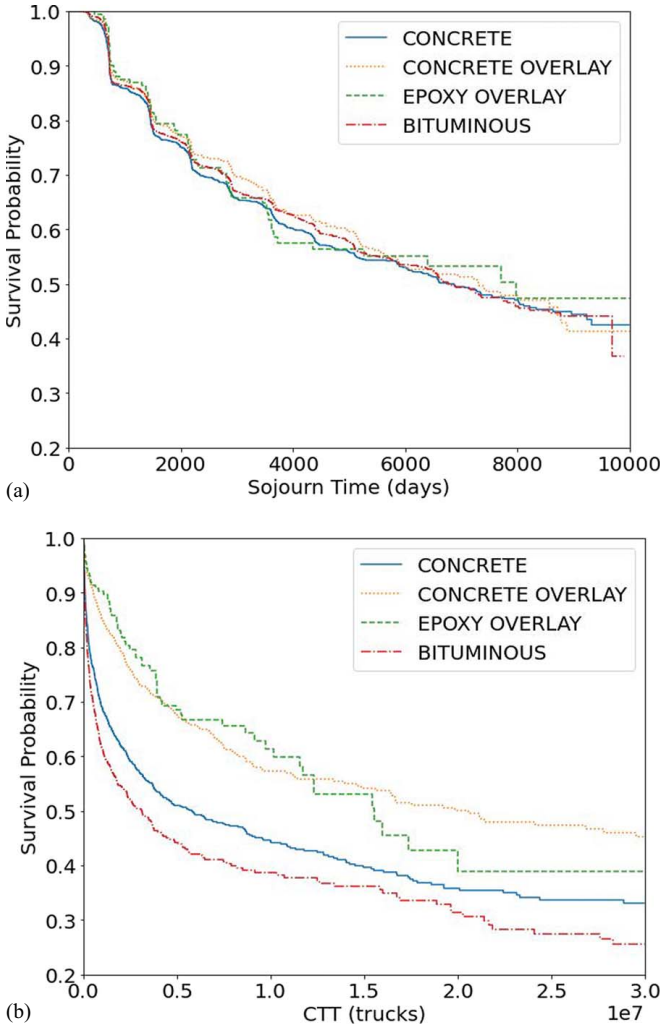

Fig. 3. Deterioration pattern with different dependent variables for deck surface types: (a) sojourn time as dependent variable; and (b) CTT as dependent variable.

nonparametric reliability for duration, t, was calculated as

$$\hat{R}(t) = \prod_i \frac{n_i - m_i}{n_i} \tag{14}$$

where n_i = number of sojourn times that are greater than or equal to time t_i; and m_i = number of sojourn times that are exactly equal to t_i.

Consider the deck surface type as an example. Expert knowledge would anticipate that bituminous overlays would be less durable than concrete. This can be observed in the usage of these materials: while 55.1% of bridges with ADTT less than 1,000 trucks/day used bituminous surface, 65.5% of bridges with ADTT larger than 1,000 trucks/day used concrete. Next, the reliability of bridge decks predicted from the data using the nonparametric K–M estimate is determined considering: (a) the sojourn time as the dependent variable, and (b) the CTT as the dependent variable. The results are shown in Fig. 3. Looking at Fig. 3(a), concrete deck surface types appear to deteriorate more quickly than others, while all bridges with different surface types share a similar deterioration pattern if the sojourn time is used as the dependent variable. This is a counterintuitive result. However, the reason for this observation is that this dependent variable does not consider that bridge decks utilizing bituminous material also typically experience lower truck traffic due to the selection bias in the overlay material. Hence, when considering CTT as the dependent variable [Fig. 3(b)], the reliability trends are more as expected: bituminous overlays have the lowest reliability and epoxy overlay has the highest reliability. Similar trends in reliability for other attributes were also observed when comparing the sojourn time with the CTT as the dependent variable. Hence, the CTT was chosen as the dependent variable for this study.

Accuracy of the AFT–GGD Model

After the dependent variable was determined, the suitability of the GGD to fit the deterioration pattern was tested and compared with the other commonly used statistical models, for example, Weibull, log-normal, log-logistic, and exponential.

First, the data set was divided into four parts based on the rebar type, for example, bare rebar type, epoxy rebar type, galvanized rebar type, and other rebar type. The survival probability curves were estimated with the K–M estimator as ground truth and different distributions were applied to fit the data. The K–M curve also includes a band of reliability that represents the robustness of the survival probability determined from the data. This curve is typically wider when fewer data are available. Fig. 4 shows the fitting curves.

Fig. 4 shows that different rebar types have different deterioration patterns; hence, a flexible distribution can help accommodate the different scenarios. Log-normal, log-logistic, and GGD achieved better performance in general compared with Weibull and exponential models, especially when the CTT was less than 5 million trucks. As the CTT increased, the differences between the fitting curves also increased. The accuracy and performance of the different distributions compared with the nonparametric K–M estimation were quantified considering three metrics: mean average error (MAE), root-mean square error (RMSE), and log-likelihood. Table 3 lists the results.

Table 3 indicates that the other distributions never outperform the GGD and often underperform. Hence, these results suggest that the flexibility of the GGD leads to better accuracy in predicting the deterioration of bridge decks.

Next, a single model that considers the rebar type as its only covariate was developed. The covariate was incorporated into the different distributions using the AFT approach and the general performance of the different distributions was evaluated considering the entire data set. Table 4 lists the results of the accuracy metrics.

As seen in Table 4, the AFT–GGD model achieved the lowest MAE and highest log-likelihood compared with the other models. Even though the RMSE of AFT–GGD was slightly lower than the log-logistic model, the general performance of the AFT–GGD was still the best. This confirmed that AFT–GGD model has a higher predictive accuracy than other commonly used statistic models in the literature.

Accuracy of the MCMC Methodology

The previous subsection showed that AFT–GGD can achieve better accuracy than other distributions, especially when many covariates exist. The estimation of this type of model is complicated due to the complex structure of the GGD and the additional parameter that must be estimated (Hirose 2000; Hwang and Huang 2002). Therefore, the MCMC method was adopted in this study to estimate the AFT–GGD model. The accuracy of MCMC was also evaluated based on the reduced model where only a single covariate is considered for convenience and simplicity.

The model parameters were estimated using: (1) a maximum likelihood estimation utilizing the Newton method (Abatzoglou and Gheen 1998), which is one of the most commonly used parameter estimation method in the literature; and (2) MCMC. A histogram plot for the samples of the coefficient for bare rebar type (Fig. 5) shows that the samples follow a normal distribution. The

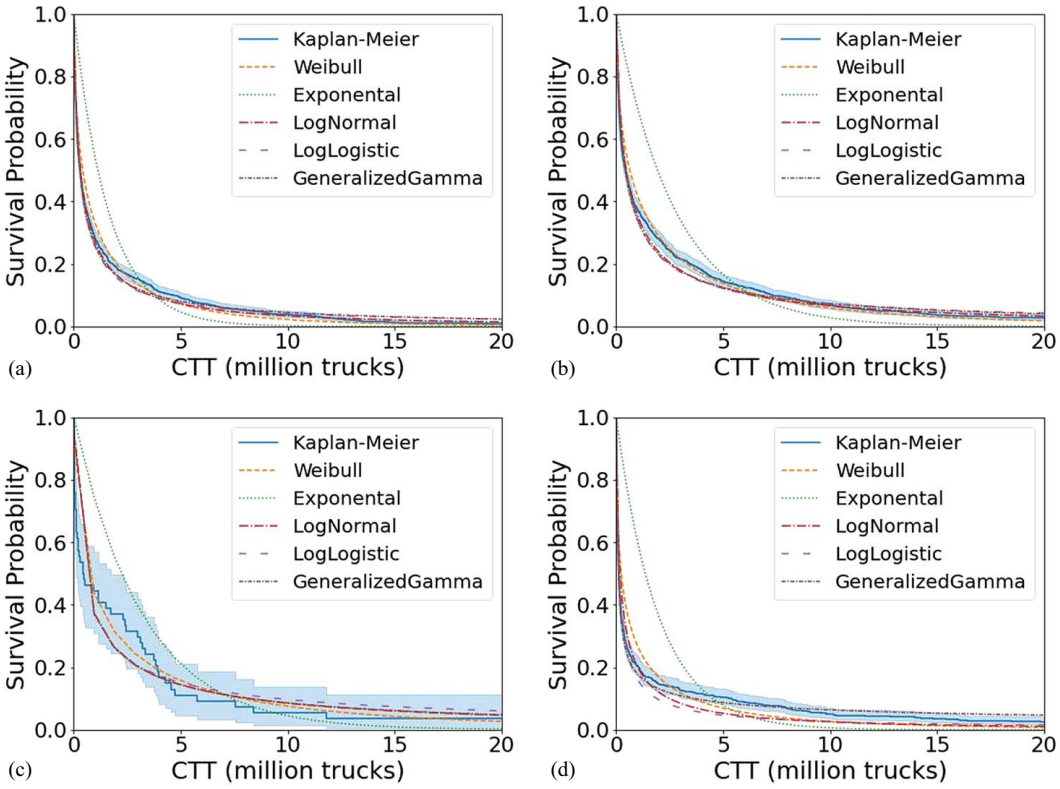

Fig. 4. Survival probability curve of different rebar types fitted to different distributions: (a) bare rebar type; (b) epoxy rebar type; (c) galvanized rebar type; and (d) other rebar types.

Table 3. Evaluation indexes of different distributions

Sub-data set	Criteria	Weibull	Exponential	Log-normal	Log-logistic	Generalized gamma
Bare rebar	MAE	0.04	0.18	**0.02**	**0.02**	**0.02**
	RMSE	0.05	0.22	**0.02**	0.03	**0.02**
	Log-likelihood	−1,248.78	−1,889.37	−1,144.68	−1,184.81	**−1,135.60**
Epoxy rebar	MAE	0.04	0.20	**0.03**	**0.03**	**0.03**
	RMSE	0.05	0.23	**0.03**	**0.03**	**0.03**
	Log-likelihood	−1,668.63	−2,360.62	−1,590.24	−1,632.52	**−1,586.27**
Galvanized rebar	MAE	**0.05**	0.22	**0.05**	**0.05**	**0.05**
	RMSE	**0.06**	0.25	**0.06**	**0.06**	**0.06**
	Log-likelihood	−80.34	−116.97	−78.23	−80.81	**−78.23**
Other rebar type	MAE	0.07	0.30	0.05	0.04	**0.02**
	RMSE	0.08	0.35	0.05	0.04	**0.02**
	Log-likelihood	−344.19	−1,000.75	−245.46	−251.01	**−180.79**

Note: The best results of model comparison are given in bold.

coefficient samples of other rebar types displayed a similar pattern, which indicated the MCMC samples converged well.

Since the MCMC method provides a distribution for each parameter, the parameters were then estimated from this method using either a maximum a posterior estimation (MAP) or simple mean. The resulting estimates can be seen in Fig. 5 as the distribution of the parameter for the bare rebar, a normal distribution fitted to the parameter distribution, and the three point-estimates of the parameter.

From Fig. 5, it can be observed that the three different point-estimates of the parameter are close. This indicates that the MCMC method can closely predict the parameter values compared with standard methods. The advantage of the MCMC method is that, along with the point estimation, it provides a distribution for the parameter, which can be used to determine bands of confidence around predictions of parameters and is also useful for updating the parameters as new data become available. Since the samples can be closely fitted to a normal distribution, the MAP estimation and mean of the sample should theoretically be identical. For the remainder of the paper, the mean of the sample distribution is used as the point estimate of each parameter.

Survival probability was determined using both the predictive model and the K–M estimation based solely on data shown in Fig. 6. In Fig. 6, the K–M estimation and MLE were calculated using the *lifelines* package in Python (Davidson-Pilon et al. 2021), along with a 95% confidence interval calculated using Greenwood's formula shown as the bounds in the figure (Cox and Oakes 1984). The MCMC method results are shown with a mean of samples estimation.

From Fig. 6, it can be seen that the predictive model had a high accuracy and closely predicted the deterioration pattern of different rebar types and was able to distinguish the influence of different

rebar types on deterioration. Note that the galvanized rebar type exhibits a larger confidence interval than do others, due to the small number of observations in this category. A confusion matrix, which shows the accuracy of predicting the sojourn time using different rebar type variables, was calculated as listed in Table 5. This matrix shows the relative error of prediction of survival for a bridge with a given rebar type using a model developed for another (or the same) rebar type. For example, if the deterioration of a bridge deck with epoxy rebar was being predicted, but the model for bare rebar was used, the relative error was observed to be 0.33. It can be seen that the model had the largest accuracy along the diagonal, which is when the correct rebar type from the data was used to predict the survival probability of the data.

Table 4. Evaluation indexes of different AFT models on the whole data set

Models	MAE	RMSE	Log-likelihood
AFT–Weibull model	0.0553	0.0707	−3359.3422
AFT–exponential model	0.2224	0.2674	−5,367.7140
AFT–log-normal model	0.0398	0.0524	−3,064.0266
AFT–log-logistic model	0.0392	**0.0514**	−3,153.5695
AFT–GGD model	**0.0371**	0.0518	**−3,020.6304**

Note: The best results of model comparison are given in bold.

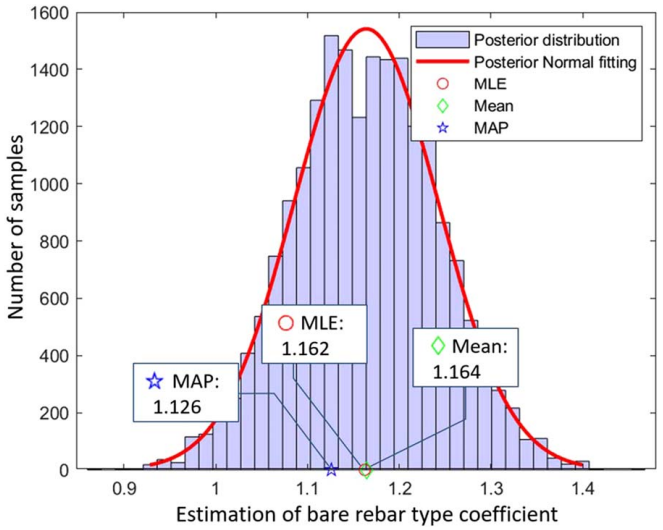

Fig. 5. Comparison of estimation results of bare rebar type.

In addition to the accuracy of the model, the stability of the parameter estimation was also compared with a maximum likelihood estimation. The distributions of the posterior samples of each parameter along with the quartiles were compared with the 95% confidence interval from MLE, as shown in Fig. 7. From Fig. 7, it can be found that the lower and upper quartiles are always within the 95% confidence intervals of MLE and achieved a tighter estimate for the shape parameters, λ and σ.

Estimation of the Full Model

Next, six full models for CR 4 through CR 9 were estimated considering all attributes. To achieve this, all data were initially included in the model and a backward elimination was performed. Finally, 41 attributes were included for various CR ratings. Using these attributes, 20,000 samples of the MCMC were generated. All the samples of each variable approximately followed a normal distribution and concentrated within a stable range. The samples' distribution indicated that those models converged well. Even though the posterior distribution represents the joint probability of the coefficient of each covariate, in this study the coefficients were found to be independent. A correlation coefficient matrix indicated that 91.25% of the pairs of coefficients had very low correlation coefficients between −0.2 and 0.2. Only a few covariates were found to be correlated, which typically were the coefficients of different realizations of the same attribute,

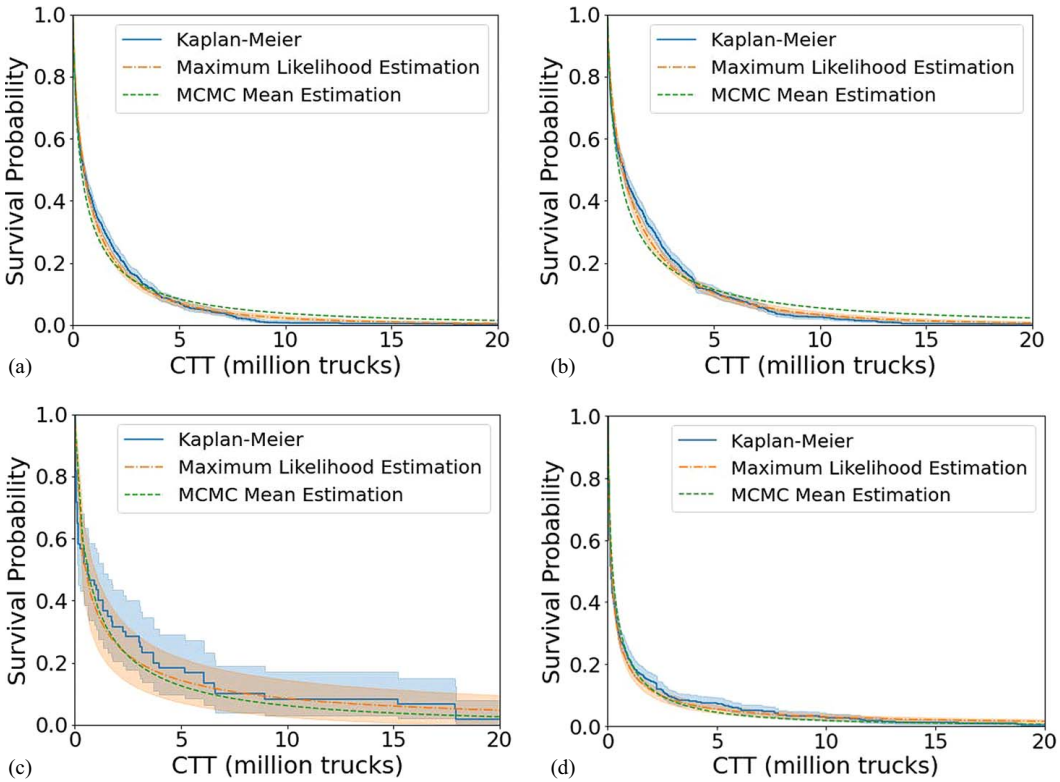

Fig. 6. Comparison of MCMC results with MLE results: (a) bare rebar type; (b) epoxy rebar type; (c) galvanized rebar type; and (d) other rebar types.

such as different main structural configurations or different district areas. Hence, covariates were treated independently, and the marginal distributions were used to estimate the coefficients. The mean of the coefficients estimated for each CR model are shown in the Appendix.

Notice that each discrete variables' coefficient was estimated considering a baseline, for example, for the CR4 model the baseline for the district variable was Districts 2 and 8. The baseline is selected as the value of an attribute that would result in a deterioration pattern most similar to the general deterioration pattern from the whole data set. Hence, the baseline is usually chosen as the value of an attribute that is most frequent in the data set. For example, for the *Deck Protection Type* variable, 57.01% of the bridges (18,171 out of 31,872) are in the *No* protection category. Thus, the *No* protection category is selected as the baselines for the accelerated failure model for all CRs. The coefficient for each variable that is not chosen as the baseline represents the ATF for that variable, that is, a positive coefficient represents a decelerated timeline and thus associate with higher reliability, and a negative coefficient represents an accelerated timeline and thus associating with lower reliability.

Attribute Reliability Analysis

The results reveal that the influence of each attribute for different condition ratings varied slightly, though the trends were consistent.

Table 5. Confusion matrix of the predictive model

		Observation			
Relative error		Bare rebar	Epoxy rebar	Galvanized rebar	Rebar baseline
Prediction	Bare rebar	**0.15**	0.46	0.33	0.48
	Epoxy rebar	0.33	**0.16**	0.22	0.70
	Galvanized rebar	0.16	0.18	**0.14**	0.59
	Rebar baseline	0.64	1.11	0.93	**0.31**

Note: Bold values are used to highlight the accuracy of the model.

In addition, since all the attributes were incorporated into the model as a binary variable (0 or 1), and the coefficient of a given attribute represented the independent influence of this attribute, the model can easily be used to understand the reliability of bridges considering multiple attributes by simply summing their coefficients. For example, when a new bridge with an epoxy rebar type is constructed in District 2, and another with a bare rebar type is built in District 5, the reliability of the two bridges can directly be compared by adding the coefficients of the relevant rebar type and district number from the model to obtain the reliability of each bridge. This feature can be used to analyze the reliability of newly constructed bridges. Some detailed results and observations from Appendix I for the specific attributes are discussed further next.

The mean value of the parameters of the *DISTRICT* attribute for each CR is plotted in Fig. 8(a), along with the error bars that represent the standard deviations of those samples. Bridges from different districts have different management strategies, environmental conditions, budgets, and traffic conditions; hence, bridge performance varied among districts. Bridges that had the highest reliability were in Districts 5 and 6, which are in eastern Pennsylvania. This distinction is most likely due to economic development and weather conditions in that location.

Fig. 8(b) shows the coefficients for different levels of the *physical makeup of main span* variable in the reliability models. In this data set, 49.9% of all bridges had a *pretensioned* physical type, which was often selected as the baseline, followed by 21.1% of bridges having a *reinforced concrete* physical type. The results show that reinforced physical type had a higher reliability than pretensioned physical type for low CRs, but the pretensioned physical type had the highest reliability for CR 9. These results are consistent with empirical observations of the data, where the reliability of pretensioned concrete is the highest initially, however, decreases more rapidly than reinforced concrete as loading increases (Dai et al. 2020). Further, the coefficients for *rolled sections* (with or without cover plates) were generally negative, implying that the

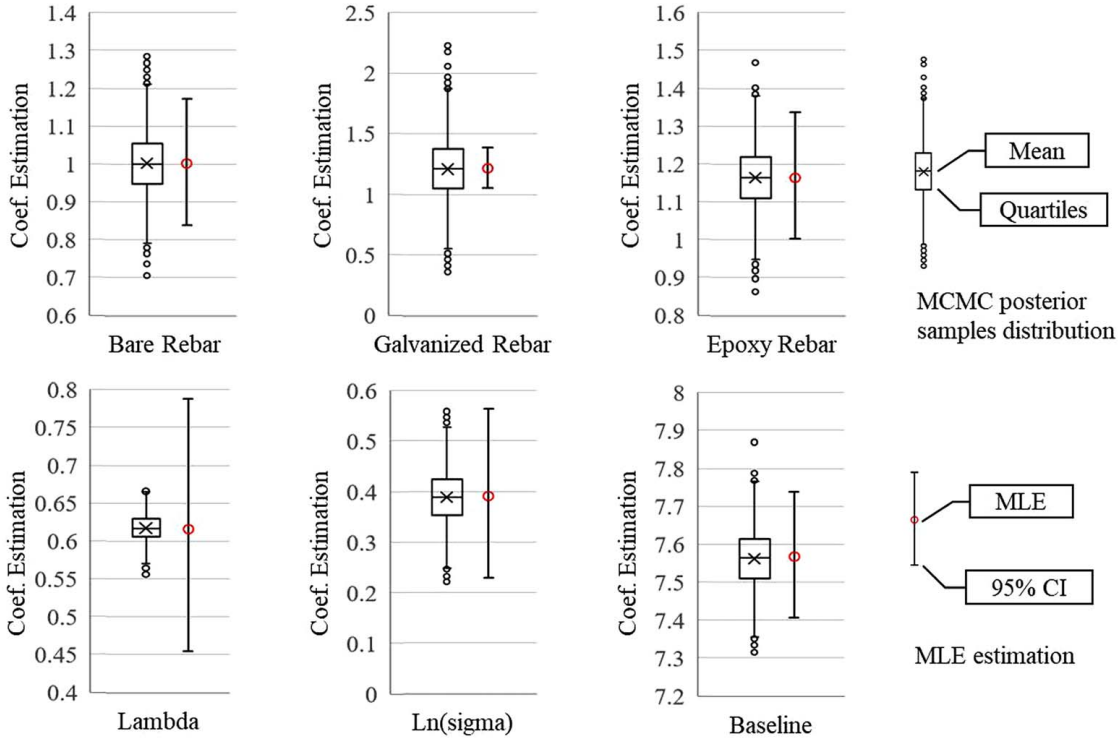

Fig. 7. Stability comparison of MCMC approach.

J. Bridge Eng., 2022, 27(4): 04022006

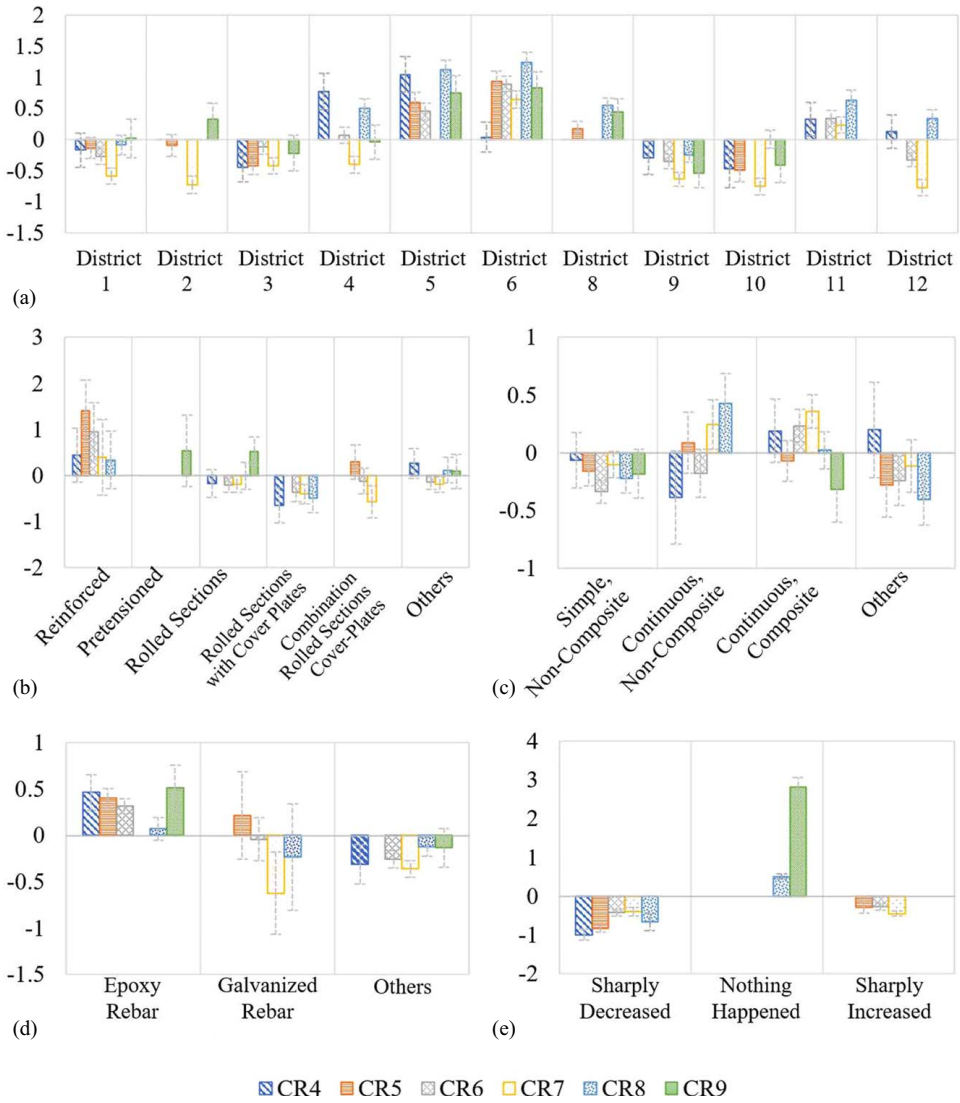

Fig. 8. Parameters of key attributes in each condition rating: (a) district; (b) physical makeup of the main span; (c) span interaction for the main span; (d) rebar type; and (e) special events.

rolled sections may not have as high reliability as pretensioned physical type in practice.

For the *span Interaction for main span*, the *simple, composite* span interaction was the most used type and, hence, was selected as the baseline. Fig. 8(c) shows that continuous span interactions for the main span of the structure were generally stronger compared with the simple, composite span intersection, and composite span interactions often lead to higher reliability than noncomposite span interactions for most CRs, that is, CR 4, CR 6, CR 7.

For the *rebar type*, bare rebar was chosen as the baseline since most bridge decks were constructed using bare rebar. The results of the coefficient estimations of rebar type suggest that epoxy rebar had the highest reliability compared with other rebar types, which is expected. Epoxy-coated rebar is used to resist corrosion, especially against exposure to deicing salts or marine environments, and can provide acceptable protection compared with bare rebar. Lab experiments have shown that epoxy-coated rebar can significantly outperform bare rebar (McCrum and Arnold 1993). Conversely, the same lab experiments also suggested that the galvanized rebar should also perform similar to epoxy-coated rebar and outperform bare rebar types, since galvanizing is a corrosion protection method where the zinc and zinc alloy coating provides both barrier and sacrificial protection to the steel. However, only 1.75% of all bridges had galvanized rebar, leading to large confidence intervals for the coefficient estimations [Fig. 8(d)].

Another interesting result was obtained for bridge decks that experienced sharp declines or increases in condition ratings, that is, a change of more than two condition ratings between two consecutive inspections. The sudden increases could be due to a maintenance or reconstruction activity, and the sudden declines could be due to an incident happening on the bridge causing it to deteriorate quickly in a short time. Fig. 8(e) shows the parameters for the baseline: only smooth transitions, sharply increase, and sharply decrease. The model results showed that after a bridge had been maintained, the performance would decline compared with a bridge deck without any sudden changes in condition rating. Further, it was observed that a sharp decrease in condition rating has a larger impact on reliability as compared with a sharp increase, which is most likely due to a controlled maintenance activity.

Bayesian Results

As new inspection data become available, the old model will require updating. In this case, Bayesian theory can be utilized to

update the parameters of the existing model. The CR 6 data set was utilized to demonstrate the proposed method.

First, the data set was divided into two parts according to the inspection date of the bridges. The first data set consisted of all the inspection data before 2000, and the second data set consisted of all the inspection data between 2000 and 2015. Another test that used the entire data set as one was also developed to compare with the two-step updated results. The number of observations that were available in each data set are given in Table 6.

First, Data set 1 was modeled as described in the *Estimating the Parameters* section using a uniform distribution as the prior distribution, and 20,000 samples are generated from the posterior distribution using the MCMC method. A normal distribution was used to fit these samples to obtain the posterior distribution (see Step 1 histograms and fitted curves in Fig. 9). Next, the fitted normal distributions for each parameter were used as the prior distribution for determining the posterior distribution using Data set 2. Again, 20,000 samples were generated from the posterior distribution, and a normal distribution was used to fit the samples to obtain the posterior distribution (see Step 2 histograms and fitted curves in Fig. 9). The results from the test using the entire data set at once are also shown in Fig. 9 (see all data histograms and fitted curves in Fig. 9) to compare the results from the updating process and direct calculation.

Fig. 9 only demonstrates four of all parameters as an illustration. From Fig. 9, it can be observed that as more data became available, the samples became more concentrated, and the interval estimation also resulted in a narrower range. The predictive accuracy of the updated model converged to the results that were estimated using the entire data set. The correlation coefficient between the results after two steps updating and the estimations using the entire data set is 0.9876, which showed that the Bayesian updating method can obtain reliable results. The Bayesian self-updating process provides more flexibility and efficiency to update the existing model when new inspection data become available, rather than re-estimating the model from scratch.

Table 6. Data set description

Data set	Censored data	Complete data	Total
1985–2000	5,404	1,301	6,705
2000–2015	5,405	2,470	7,875
1985–2015 (entire data set)	7,264	3,827	11,091

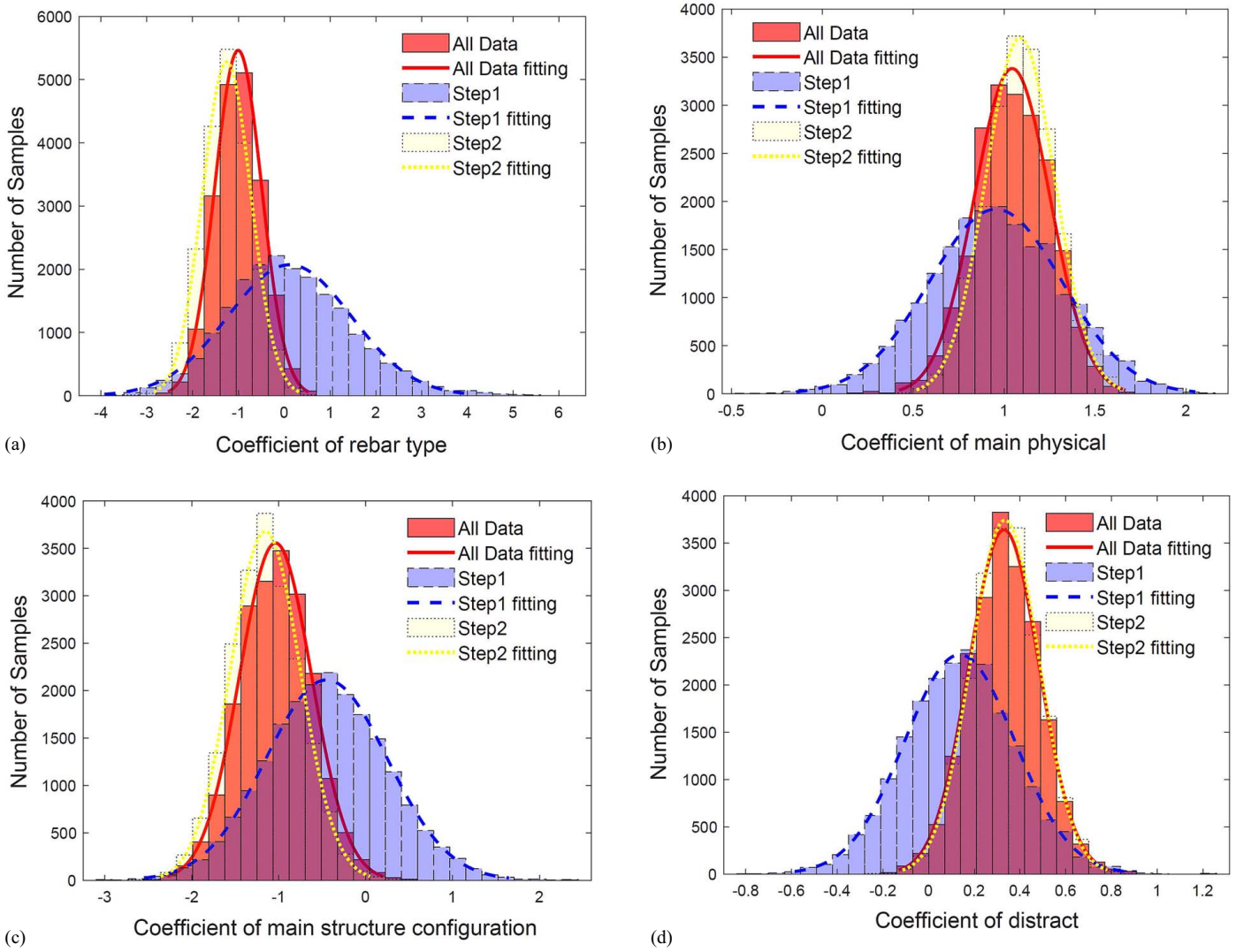

Fig. 9. Bayesian updating results: (a) coefficient of rebar type; (b) coefficient of main physical; (c) coefficient of main structure configuration; and (d) coefficient of distract.

Conclusions

This paper advances the knowledge in infrastructure deterioration modeling by considering a more powerful distribution, that is, the generalized gamma distribution, which utilizes a Bayesian inference-based parameter estimation approach. The proposed AFT–GGD model has the flexibility to model different shapes of deterioration curves and therefore was able to achieve a higher predictive accuracy than were traditional statistical models, such as Weibull, log-normal, log-logistic, and exponential distributions-based models. This was shown using a reduced model that only considered rebar type as a covariate, and the results suggested that the AFT–GGD model had a log-likelihood of −3,020, whereas the commonly used AFT–Weibull model had a log-likelihood of −3,359 on the same data set. Other distributions were not able to adapt to the different deterioration patterns that were observed when considering different rebar types. However, this flexibility comes at the cost of complexity of estimating the model parameters. Therefore, a heuristic approach, namely the MCMC sampling method, was adopted to estimate the parameters, and several computational issues were addressed in this study as well. The results suggest that the MCMC can achieve a comparable accuracy with the MLE and obtain stable estimations of the model parameters, since on a reduced model both the upper and lower quartiles of the posterior samples are within the 95% confidence interval of MLE. Further, the results of this paper suggest that choosing the cumulative truck load (CTT) as the dependent variable instead of a traditional solely time-based dependent variable can improve the predictions of the impact of covariates on the deterioration process. The CTT model emphasizes the impact of aging and traffic load simultaneously, and therefore the reliability analysis based on this dependent variable is more consistent with engineering judgment. For example, when using CTT as the dependent variable, the epoxy overlay had the highest reliability followed by the concrete overly and the bituminous overlay. In an equivalent time-based model, this order was not preserved. Similar predictive performance improvements were observed for other attributes as well. The final model that includes all attributes suggest that the district, physical makeup of main span, span interaction of main span, and rebar type have significant impact on the deterioration process of bridges in Pennsylvania.

Some limitations exist in this study and should be studied in the future. The mathematical solution of the parameter estimates for the AFT–GGD are difficult to calculate. Even though heuristic solutions theoretically converge to the optimal solution, the accuracy and efficiency of those solutions depend greatly on the chosen hyperparameters of the algorithm. Hence, further improvements can be done to get parameter estimates with tighter confidence intervals. Also, even though the Bayesian estimation can be used to update the model when new data are available, this is purely data-driven. Incorporation of expert knowledge into this updating process should be studied further. In addition, the proposed models could be used on different data sets to ensure that similar findings hold when considering different databases.

Appendix I. Parameter Estimations of the Full Model

Attributes	CR 4	CR 5	CR 6	CR 7	CR 8	CR 9
District						
District 1	−0.172	−0.1381	−0.2728	−0.5901	−0.0894	0.0162
District 2	*	−0.0997	*	−0.7327	*	0.327
District 3	−0.4446	−0.4267	−0.1247	−0.4232	*	−0.2198
District 4	0.7709	*	0.0649	−0.4061	0.506	−0.0398
District 5	1.0466	0.598	0.4514	*	1.1258	0.7528
District 6	0.0359	0.9389	0.8934	0.641	1.2452	0.8245
District 8	*	0.1756	*	*	0.5437	0.4424
District 9	−0.2991	*	−0.3522	−0.6383	−0.2432	−0.5398
District 10	−0.4664	−0.4978	*	−0.7578	−0.0016	−0.4088
District 11	0.3295	*	0.3404	0.2328	0.6338	*
District 12	0.1242	*	−0.3278	−0.7794	0.338	*
Main materials type						
Steel	*	*	*	*	*	−0.3919
Concrete (cast in place)	0.2031	−0.2634	−0.267	0.678	0.3162	*
Concrete (precast)	—	−0.5625	−0.4967	0.4	−0.3127	—
Prestressed precast concrete	*	*	*	*	−0.1634	−0.7049
Concrete encased steel	0.1904	0.4508	0.1754	0.4344	0.1246	—
Physical makeup of main span of structure						
Reinforced	0.4344	1.4082	0.9421	0.3849	0.3278	*
Pretensioned	*	*	*	*	*	0.5282
Rolled sections	−0.1781	*	−0.2153	−0.1943	−0.0124	0.5223
Rolled sections with cover plates	−0.6588	*	−0.3695	−0.4118	−0.5	—
Combination, rolled Sections, or Cover plates	—	0.2895	−0.1294	−0.578	—	—
Other	0.2566	*	−0.1561	−0.1998	0.11	0.0811
Span interaction for main span of structure						
Simple, composite	*	*	*	*	*	*
Simple, noncomposite	−0.0664	−0.1583	−0.3387	−0.1015	−0.2207	−0.184
Continuous, noncomposite	−0.3865	0.089	−0.1764	0.2442	0.4293	—
Continuous, composite	0.1907	−0.0733	0.2347	0.3572	0.0206	−0.32
Other	0.1987	−0.2811	−0.243	−0.1141	−0.4062	—
Structural configuration for main span of structure						
Slab (solid)	−0.7481	−0.9218	−0.8948	−0.9919	−0.4654	0.1931
T beams	−0.2448	−0.5426	−0.3899	−0.848	−0.247	0.8732
I beams	*	*	*	*	0.1833	*
Box beam, single	−0.2722	−0.2242	−0.4843	−0.5586	*	0.2272
Box beam, adj	−0.4231	−0.485	−0.6576	−0.6051	−0.3807	−0.2772
I-welded beams	—	−1.1168	−0.538	−0.7838	−0.2569	-
Girder weld/deck	−0.5607	0.1753	0.2236	−0.0005	*	-
Deck protection type						
No	*	*	*	*	*	*
Epoxy-coated reinforcing	*	*	*	0.4535	0.4208	0.2034
Galvanized reinforcing	—	−0.0321	*	0.8791	0.6218	-
Deck rebar type						
Bare rebar	*	*	*	*	*	*
Epoxy rebar	0.464	0.4066	0.3161	*	0.0724	0.5141
Galvanized rebar	—	0.2146	−0.0435	−0.6243	−0.233	-
Others	−0.311	—	−0.2592	−0.3624	−0.1209	−0.1343
Main bridge spans (number of spans in main unit)						
1	*	*	0.1717	0.2323	*	*
2	−0.0423	−0.2493	*	*	−0.1913	0.2646
3	0.9023	0.7065	0.9246	0.7042	0.4596	0.8411
4	0.1244	−0.2311	*	0.1665	0.1174	−0.0462
5	1.224	0.3203	0.295	*	0.0645	—
6	—	—	0.0878	−0.2673	—	—
Waterproofing membrane on bridge main span						
No	*	*	*	*	*	*

(*Continued*.)

Attributes	CR 4	CR 5	CR 6	CR 7	CR 8	CR 9
Preformed fabric	0.0913	0.558	*	0.2054	0.406	0.5369
Epoxy	—	—	—	−0.0879	—	—
Other	—	−0.3782	−0.7985	−0.8029	—	—
Wearing surface types on bridge main span						
Concrete	*	*	*	*	*	*
Concrete overlay	0.462	0.6124	0.6774	0.5288	0.6413	0.5869
Epoxy overlay	0.7728	0.9731	0.7558	0.8091	1.0521	—
Bituminous	0.4119	*	0.4016	0.4239	0.4598	0.5825
Special events						
Sharply decrease	−0.9948	−0.8328	−0.4298	−0.403	−0.6643	*
Nothing happened	*	*	*	*	0.5094	2.803
Sharply increase	*	−0.293	−0.2683	−0.4494	*	*
Length	0.1736	0.3423	0.3293	0.4505	0.1212	0.653
Deck width	10.2289	9.5222	8.4817	10.4584	10.5333	11.322
Ln (Sigma)	0.4118	0.4726	0.4288	0.4351	0.3678	0.4232
Lambda	0.6226	0.3328	0.4375	0.4071	0.3318	0.2827
Beta_0	−3.6452	−4.2849	−3.9917	−4.4316	−6.2533	−7.4602

"*" implies the baseline for each model; "—" implies that not enough data were available to include in the model (denotes less than 500).

Appendix II. Derivation of AFT–GGD Model

The probability density function (PDF) of a standard GGD is shown as

$$f(t)=\frac{\beta}{\Gamma(k)\theta}\left(\frac{t}{\theta}\right)^{k\theta-1}e^{-\left(\frac{t}{\theta}\right)^{\beta}} \tag{15}$$

where k, β, θ = parameters of the distribution; t = independent variable; $\Gamma(k)$ = gamma function as shown in

$$\Gamma(k)=\int_0^{\infty}s^{k-1}e^{-s}ds \tag{16}$$

The standard GGD is simple, however the parameters cannot be easily estimated. Hence, this was reparametrized according to Lawless (Lawless 2011), using new parameters μ, σ, λ as

$$\mu=\ln(\theta)+\frac{1}{\beta}\ln\left(\frac{1}{\lambda^2}\right) \tag{17}$$

$$\sigma=\frac{1}{\beta\sqrt{k}} \tag{18}$$

$$\lambda=\frac{1}{\sqrt{k}} \tag{19}$$

Hence, the updated PDF of the generalized gamma distribution with the new parameters is

$$f(t)=\begin{cases}\dfrac{|\lambda|}{\sigma t}\dfrac{1}{\Gamma\left(\frac{1}{\lambda^2}\right)}e^{\left[\frac{\lambda\frac{\ln(t)-\mu}{\sigma}+\ln\left(\frac{1}{\lambda^2}\right)-e^{\lambda\frac{\ln(t)-\mu}{\sigma}}}{\lambda^2}\right]} & \lambda\neq 0\\ \dfrac{1}{t\sigma\sqrt{2\pi}}e^{-\frac{1}{2}\left(\frac{\ln(t)-\mu}{\sigma}\right)^2} & \lambda=0\end{cases} \tag{20}$$

Then, the reliability function can be determined as

$$R(t)=1-\int_0^t f(x)dx=\begin{cases}1-\Gamma_I\left(\dfrac{1}{\lambda^2};\dfrac{e^{\lambda\frac{\ln(t)-\mu}{\sigma}}}{\lambda^2}\right) & \lambda>0\\ 1-\Phi\left(\dfrac{\ln(t)-\mu}{\sigma}\right) & \lambda=0\\ \Gamma_I\left(\dfrac{1}{\lambda^2};\dfrac{e^{\lambda\frac{\ln(t)-\mu}{\sigma}}}{\lambda^2}\right) & \lambda<0\end{cases} \tag{21}$$

Note that the GGD can be simplified to other well-known distributions, such as the Weibull distribution ($\lambda=1$), exponential distribution ($\lambda=1$ & $\sigma=1$), lognormal distribution ($\lambda=0$), or gamma distribution ($\lambda=\sigma$).

To incorporate the covariates into the model, first the independent variable t was normalized to $Z(t)$:

$$Z(t)=\frac{\ln(t)-\mu}{\sigma}=\frac{1}{\sigma}\ln\left(\frac{t}{\mu}\right) \tag{22}$$

From this normalized expression, it was found that μ is the scale parameter and λ, σ are shape parameters. The scale parameter, μ, could be replaced with an exponential linear combination of covariates as

$$\mu=e^{\boldsymbol{\beta x}} \tag{23}$$

Then, the GGD became an AFT–GGD, the PDF becomes

$$f(t,\boldsymbol{x}|\sigma,\lambda,\boldsymbol{\beta})=\begin{cases}\dfrac{|\lambda|}{\sigma t}\dfrac{1}{\Gamma\left(\frac{1}{\lambda^2}\right)}e^{\left[\frac{\lambda\frac{\ln(t)-e^{\boldsymbol{\beta x}}}{\sigma}+\ln\left(\frac{1}{\lambda^2}\right)-e^{\lambda\frac{\ln(t)-e^{\boldsymbol{\beta x}}}{\sigma}}}{\lambda^2}\right]} & \lambda\neq 0\\ \dfrac{1}{t\sigma\sqrt{2\pi}}e^{-\frac{1}{2}\left(\frac{\ln(t)-e^{\boldsymbol{\beta x}}}{\sigma}\right)^2} & \lambda=0\end{cases} \tag{24}$$

Data Availability Statement

The data that support the findings of this study are available from the Pennsylvania DOT (PennDOT). Restrictions apply to the availability of these data, which were used under license for this study. Data are available from the authors with the permission of PennDOT. All codes used during the study are available in a repository online (Google Drive 2022).

Acknowledgments

This work was supported by funds available through Center for Integrated Asset Management for Multimodal Transportation Infrastructure Systems (CIAMTIS): Region 3 University Transportation Center. The content of this paper reflects solely the views of the authors, who are responsible for the facts and the accuracy of the data

presented herein. The contents do not necessarily reflect the official views or policies of the U.S. DOT.

References

Abatzoglou, T. J., and G. O. Gheen. 1998. "Range, radial velocity, and acceleration MLE using radar LFM pulse train." *IEEE Trans. Aerosp. Electron. Syst.* 34: 1070–1083. https://doi.org/10.1109/7.722676.

Agarwal, S. K., and S. L. Kalla. 1996. "A generalized gamma distribution and its application in reliabilty." *Commun. Stat. Theory Methods* 25: 201–210. https://doi.org/10.1080/03610929608831688.

Agrawal, A. K., A. Kawaguchi, and Z. Chen. 2010. "Deterioration rates of typical bridge elements in New York." *J. Bridge Eng.* 15: 419–429. https://doi.org/10.1061/(ASCE)BE.1943-5592.0000123.

Barone, G., and D. M. Frangopol. 2014. "Reliability, risk and lifetime distributions as performance indicators for life-cycle maintenance of deteriorating structures." *Reliab. Eng. Syst. Saf.* 123: 21–37. https://doi.org/10.1016/j.ress.2013.09.013.

Bayes, C. L., and M. D. Branco. 2007. "Bayesian inference for the skewness parameter of the scalar skew-normal distribution." *Braz. J. Probab. Stat.* 21: 141–163.

Beck, J. L., and S.-K. Au. 2002. "Bayesian updating of structural models and reliability using Markov Chain Monte Carlo simulation." *J. Eng. Mech.* 128: 380–391. https://doi.org/10.1061/(ASCE)0733-9399(2002)128:4(380).

Black, M., A. T. Brint, and J. R. Brailsford. 2005. "Comparing probabilistic methods for the asset management of distributed items." *J. Infrastruct. Syst.* 11: 102–109. https://doi.org/10.1061/(ASCE)1076-0342(2005)11:2(102).

Butt, A. A. 1991. "Application of Markov process to pavement management systems at network level." Ph.D. thesis, Dept. of Civil Engineering, Univ. of Illinois at Urbana-Champaign.

Cohen, A. C., and B. J. Whitten. 2020. *Parameter estimation in reliability and life span models*. Boca Raton, FL: CRC Press.

Cox, C., H. Chu, M. F. Schneider, and A. Muñoz. 2007. "Parametric survival analysis and taxonomy of hazard functions for the generalized gamma distribution." *Stat. Med.* 26: 4352–4374. https://doi.org/10.1002/sim.2836.

Cox, D. R., and D. Oakes. 1984. *Analysis of survival data*. Boca Raton, FL: CRC Press.

Dai, L., H. Bian, L. Wang, M. Potier-Ferry, and J. Zhang. 2020. "Prestress loss diagnostics in pretensioned concrete structures with corrosive cracking." *J. Struct. Eng.* 146: 04020013. https://doi.org/10.1061/(ASCE)ST.1943-541X.0002554.

Davidson-Pilon, C., et al. 2021. "CamDavidsonPilon/lifelines: v0.25.8." *Zenodo*. https://doi.org/10.5281/zenodo.4457577.

de Melo e Silva, F., T. J. Van Dam, W. M. Bulleit, and R. Ylitalo. 2000. "Proposed pavement performance models for local government agencies in Michigan." *Transp. Res. Rec.* 1699: 81–86. https://doi.org/10.3141/1699-11.

de Pascoa, M. A. R., E. M. M. Ortega, and G. M. Cordeiro. 2011. "The Kumaraswamy generalized gamma distribution with application in survival analysis." *Stat. Methodol.* 8: 411–433. https://doi.org/10.1016/j.stamet.2011.04.001.

Enright, M. P., and D. M. Frangopol. 1999. "Condition prediction of deteriorating concrete bridges using Bayesian updating." *J. Struct. Eng.* 125: 1118–1125. https://doi.org/10.1061/(ASCE)0733-9445(1999)125:10(1118).

FHWA (Federal Highway Administration). 2016. "Traffic Monitoring Guide – Policy." Federal Highway Administration [WWW Document]. Accessed March 10, 2021. https://www.fhwa.dot.gov/policyinformation/tmguide/.

Gomes, O., C. Combes, and A. Dussauchoy. 2008. Parameter estimation of the generalized gamma distribution". *Math. Comput. Simul.* 79: 955–963. https://doi.org/10.1016/j.matcom.2008.02.006

Google Drive. 2022. WWW Document. Accessed January 11, 2022. https://drive.google.com/file/d/1hZQa4-DEWMAo27ufBW8E6KJV-1QmVz7Y/view?usp=sharing.

Hirose, H. 2000. "Maximum likelihood parameter estimation by model augmentation with applications to the extended four-parameter generalized gamma distribution." *Math. Comput. Simul* 54: 81–97. https://doi.org/10.1016/S0378-4754(00)00201-9.

Howard, R. A. 2007. "Dynamic probabilistic systems." In Vol. 2 of *Semi-Markov and decision processes*. 1st ed. Mineola, NY: Dover Publications.

Hsein Juang, C., Z. Luo, S. Atamturktur, and H. Huang. 2013. "Bayesian updating of soil parameters for braced excavations using field observations." *J. Geotech. Geoenviron. Eng.* 139: 395–406. https://doi.org/10.1061/(ASCE)GT.1943-5606.0000782.

Hwang, T.-Y., and P.-H. Huang. 2002. "On new moment estimation of parameters of the gamma distribution using its characterization." *Ann. Inst. Stat. Math.* 54: 840–847. https://doi.org/10.1023/A:1022471620446.

Kaplan, E. L., and P. Meier. 1958. "Nonparametric estimation from incomplete observations." *J. Am. Stat. Assoc.* 53: 457–481. https://doi.org/10.1080/01621459.1958.10501452.

Kleiber, C., and S. Kotz. 2003. *Statistical size distributions in economics and actuarial sciences*. Hoboken, NJ: Wiley.

Kobayashi, K., K. Kaito, and N. Lethanh. 2010. "Deterioration forecasting model with multistage weibull hazard functions." *J. Infrastruct. Syst.* 16: 282–291. https://doi.org/10.1061/(ASCE)IS.1943-555X.0000033.

Lawless, J. F. 2011. *Statistical models and methods for lifetime data*. Hoboken, NJ: Wiley.

Manafpour, A., I. Guler, A. Radlińska, F. Rajabipour, and G. Warn. 2018. "Stochastic analysis and time-based modeling of concrete bridge deck deterioration." *J. Bridge Eng.* 23: 04018066. https://doi.org/10.1061/(ASCE)BE.1943-5592.0001285.

Manning, W. G., W. G. Manning, A. Basu, and J. Mullahy. 2002. *Modeling costs with generalized gamma regression*. Chicago: Univ. of Chicago.

McCrum, R. L., and C. J. Arnold. 1993. *Evaluation of simulated bridge deck slabs using uncoated, galvanized, and epoxy coated reinforcing steel*. Washington, DC: DOT.

Mishalani, R. G., and S. M. Madanat. 2002. "Computation of infrastructure transition probabilities using stochastic duration models." *J. Infrastruct. Syst.* 8: 139–148. https://doi.org/10.1061/(ASCE)1076-0342(2002)8:4(139).

Nasrollahi, M., and G. Washer. 2015. "Estimating inspection intervals for bridges based on statistical analysis of national bridge inventory data." *J. Bridge Eng.* 20: 04014104. https://doi.org/10.1061/(ASCE)BE.1943-5592.0000710.

O'Leary, N., B. C. Chauhan, and P. H. Artes. 2012. "Visual field progression in glaucoma: Estimating the overall significance of deterioration with permutation analyses of pointwise linear regression (PoPLR)." *Invest. Ophthalmol. Vis. Sci.* 53: 6776–6784. https://doi.org/10.1167/iovs.12-10049.

PennDOT (Pennsylvania, Department of Transportation, Bureau of Design). 2009. *Bridge Management System 2 (BMS2) coding manual: office version*. Harrisburg, PA: PennDOT.

PennDOT (Pennsylvania, Department of Transportation). 2019 "Results." [WWW Document]. Accessed March 2, 2020. https://www.penndot.gov/about-us/Results/Pages/index.html.

Sobanjo, J., P. Mtenga, and M. Rambo-Roddenberry. 2010. "Reliability-based modeling of bridge deterioration hazards." *J. Bridge Eng.* 15: 671–683. https://doi.org/10.1061/(ASCE)BE.1943-5592.0000074.

Sobanjo, J. O. 2011. "State transition probabilities in bridge deterioration based on Weibull sojourn times." *Struct. Infrastruct. Eng.* 7: 747–764. https://doi.org/10.1080/15732470902917028.

Stacy, E. W., and G. A. Mihram. 1965. "Parameter estimation for a generalized gamma distribution." *Technometrics* 7: 349–358. https://doi.org/10.1080/00401706.1965.10490268.

Straub, D., and I. Papaioannou. 2015. "Bayesian updating with structural reliability methods." *J. Eng. Mech.* 141: 04014134. https://doi.org/10.1061/(ASCE)EM.1943-7889.0000839.

Tabatabai, H., M. Tabatabai, and C.-W. Lee. 2011. "Reliability of bridge decks in Wisconsin." *J. Bridge Eng.* 16: 53–62. https://doi.org/10.1061/(ASCE)BE.1943-5592.0000133.

Taflanidis, A. A., and I. Gidaris. 2013. "Health monitoring and Bayesian updating of deteriorating bridge infrastructures." In *Structures Congress 2013: Bridging your Passion with Your Profession*, edited by B. J. Leshko and J. McHugh, 398–409. Reston, VA: ASCE.

Thomas, O., and J. Sobanjo. 2013. "Comparison of Markov chain and semi-Markov models for crack deterioration on flexible pavements." *J. Infrastruct. Syst.* 19: 186–195. https://doi.org/10.1061/(ASCE)IS.1943-555X.0000112.

Wei, L. J. 1992. "The accelerated failure time model: A useful alternative to the cox regression model in survival analysis." *Stat. Med.* 11: 1871–1879. https://doi.org/10.1002/sim.4780111409.

Yang, Y.-J., W. Wang, X.-Y. Zhang, Y.-L. Xiong, and G.-H. Wang. 2018. "Lifetime data modeling and reliability analysis based on modified weibull extension distribution and Bayesian approach." *J Mech Sci Technol* 32: 5121–5126. https://doi.org/10.1007/s12206-018-1009-8.

Zhang, W., and P. L. Durango-Cohen. 2014. "Explaining heterogeneity in pavement deterioration: Clusterwise linear regression model." *J. Infrastruct. Syst.* 20: 04014005. https://doi.org/10.1061/(ASCE)IS.1943-555X.0000182.

Zhu, W., M. Fouladirad, and C. Bérenguer. 2015. "Condition-based maintenance policies for a combined wear and shock deterioration model with covariates." *Comput. Ind. Eng.* 85: 268–283. https://doi.org/10.1016/j.cie.2015.04.005.